

Control of non-Markovian effects in the dynamics of polaritons in semiconductor microcavities

F. J. Rodríguez and L. Quiroga

Departamento de Física, Universidad de los Andes, A. A. 4976, Bogotá D. C., Colombia

C. Tejedor

Departamento de Física Teórica de la Materia Condensada, Universidad Autónoma de Madrid, Cantoblanco, E-28049, Madrid, Spain

M. D. Martín and L. Viña

Departamento de Física de Materiales C-IV, Universidad Autónoma de Madrid, Cantoblanco, E-28049, Madrid, Spain

R. André

Group Nanophysique et Semiconducteurs (CEA-CNRS), Institut NEEL-CNRS, BP166, F-38402 Grenoble Cedex 9, France

(Received 7 March 2008; revised manuscript received 30 May 2008; published 11 July 2008)

We report on time-resolved photoluminescence from semiconductor microcavities showing that an optically controllable mechanism exists to turn on and off memory effects in a polariton system. By increasing the laser pumping pulse intensity resonantly exciting the upper polariton branch, we observe revivals of the decaying time-resolved photoluminescence signal, a manifestly non-Markovian behavior of the optically active lower branch polaritons. Based on an open quantum system approach we perform a comprehensive analytical and numerical study of the optically active polaritons to confirm the origin of the observed features. Our findings show that negative detunings and strong excitation should occur simultaneously for memory effects to take place.

DOI: [10.1103/PhysRevB.78.035312](https://doi.org/10.1103/PhysRevB.78.035312)

PACS number(s): 78.66.Hf, 71.36.+c, 42.65.Sf, 78.47.-p

I. INTRODUCTION

Semiconductor microcavities (SM) have attracted a great deal of attention in recent years due to the opportunity they bring to create and manipulate, in a controlled way, many-boson systems in a solid-state environment.^{1,2} Bose-Einstein condensation signatures of radiation-matter quasiparticles (polaritons) have been recently identified in such systems.³⁻⁶ On the other hand, due to the rich possibilities of tailoring the matter-radiation interaction in SM, optically controlled dynamics of elementary electronic excitations is within reach. In particular, the understanding of the ultrafast dynamics of polaritons becomes crucial for interpreting important quantum control experiments in SM as it has been demonstrated recently.⁷ A convenient and versatile way of monitoring the ultrafast dynamics of polaritons is provided by time-resolved photoluminescence (tr-PL) experiments.

Here we focus our attention on II-VI SM where a strong exciton-LO-phonon coupling produces a rapid relaxation for nonresonantly created polaritons, with large excess energies.⁸ It has been reported that, under certain conditions, tr-PL following a nonresonant pulsed excitation of a CdTe-based microcavity shows an oscillatory emission dynamics strongly depending on the detuning and the initial excitation density.⁹ Furthermore, spin-related effects have been observed when the tr-PL is analyzed into its co- and cross-polarized components after excitation with circularly polarized pulses.^{10,11} The nonlinear coupling of optically active and dark states has been invoked as a possible mechanism to explain existing experimental results.¹² However, these unusual experimental features still seem to challenge conventional theoretical approaches.

Under resonant optical excitation SM exhibit a rich variety of coherent nonlinear optical properties dominated by

polariton parametric interactions.¹³ By contrast, for off-resonance as well as incoherent pumping conditions, monotonic behaviors are expected and theories for their explanation rely on the Born-Markov approximation to describe the polariton dynamics.^{14,15} The main feature of these approaches is to neglect memory effects, that is, the behavior of the polariton system at some time t is only determined by its configuration precisely at the same time. The validity of this assumption requires the environment characteristic correlation time to be small as compared to the relaxation time of the system. The fingerprint of a Markov process is an exponential decay, while deviations from a Markovian behavior cause a nonexponential time evolution, with eventually superimposed oscillations implying some degree of correlation between the quantum system and its environment.

The main purpose of the present paper is to describe an optically controllable mechanism of memory effects in SM and to report on tr-PL results which provide its quantitative verification. Several parameters may be used to control the presence or absence of memory effects in the dynamics of a polariton system. Some of them are of a static nature, such as the detuning between the cavity optical mode and the bare exciton resonance, whereas others are of a dynamic nature, such as the intensity of the optical pumping. Here we emphasize on the importance of the latter ones.

The analysis is carried out within the framework of the theory of open quantum systems. In the usual scenario for studying open quantum systems, a central system of interest is *directly* coupled to a large system usually labeled as the bath. In contrast, here we consider instead a three-system framework: the quantum system of interest (the emitting polaritons), a high-energy (excitonlike) polariton bath and an intermediate system (at the “bottleneck” region). The last system provides control over the *indirect* coupling between

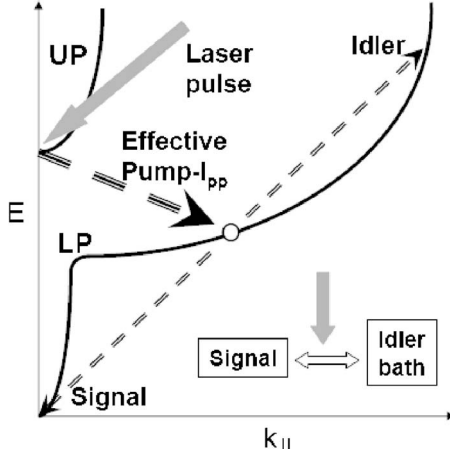


FIG. 1. Schematic representation of different polariton subsystems. Inset: two systems, signal and idler, indirectly coupled by an intensity-dependent strength.

optically active polaritons and the bath of high-energy polaritons. We show that initial excitation intensity behaves as a controllable memory mechanism for producing a rich variety of features in tr-PL signals. Spin effects are not included in the present study.

The paper is organized as follows: In Section II we present our three-coupled system model. We start by briefly discussing some aspects of a masterlike equation approach with memory effects that may provide insights on the proper dynamics of the emitting polariton system. However, polariton-polariton interactions together with polariton-loss effects are hard to include and thus make this simple approach impractical to provide an appropriate description of the problem. In order to obtain a good quantitative agreement with experimental data a microscopic Heisenberg-Langevin approach, including memory effects, has been adopted.¹⁶ In Section III we present and discuss the experimental data, which corroborate our theoretical predictions. A summary is presented in Section IV.

II. THEORETICAL BACKGROUND

A. Model

After their creation in the upper polariton (UP) branch by a pulsed laser, polaritons rapidly relax to the lower polariton (LP) branch states. Once in the LP branch, one of the main mechanisms for polariton scattering in SM is the extremely efficient parametric downconversion. By this process two polaritons are simultaneously scattered: One of them goes to a $\vec{k} \sim 0$ or “signal” particle state while the other one (conserving energy and linear momentum) goes to a high $|\vec{k}|$ excitonlike state, the so-called “idler” particle state. Thus, we start by identifying three regions of interest in the LP branch, as sketched in Fig. 1: (i) The bottom of the trap (signal states), $\vec{k} \sim 0$, with energy dispersion $E(\vec{k})$, described by operators $a_{\vec{k}}$; (ii) the intermediate or bottleneck polariton region, described by operators $c_{\vec{k}}$ and energy dispersion $\epsilon(\vec{k})$, where polaritons accumulate after a rapid relaxation from the

UP branch, and finally (iii) the excitonlike bath (idler states) described by operators $b_{\vec{k}}$ and energy dispersion $\omega(\vec{k})$. The Hamiltonian is then given by ($\hbar=1$) (Ref. 14),

$$H = \sum_{\vec{k}} E(\vec{k}) a_{\vec{k}}^{\dagger} a_{\vec{k}} + \sum_{\vec{k}} \omega(\vec{k}) b_{\vec{k}}^{\dagger} b_{\vec{k}} + \sum_{\vec{k}} \epsilon(\vec{k}) c_{\vec{k}}^{\dagger} c_{\vec{k}} + H_{XP} + H_{SI}. \quad (1)$$

In the present model polaritons are to be described by boson operators linearly interacting with a large boson bath (excitons). The polariton-polariton interaction term is given by

$$H_{XP} = \sum_{\vec{k}, \vec{k}', \vec{k}_1, \vec{k}_2} \tilde{V}(\vec{k}, \vec{k}', \vec{k}_1, \vec{k}_2) a_{\vec{k}}^{\dagger} b_{\vec{k}}^{\dagger} c_{\vec{k}_1}^{\dagger} c_{\vec{k}_2} + \text{H.c.}, \quad (2)$$

where $\tilde{V}(\vec{k}, \vec{k}', \vec{k}_1, \vec{k}_2)$ accounts for the polariton-polariton coupling and H.c. means Hermitian conjugate. Since a large population of polaritons can condense at the bottom of the trap in the LP branch, $\vec{k} \sim 0$, a self-interaction term has to be included as given by

$$H_{SI} = V_0 a_0^{\dagger} a_0^{\dagger} a_0 a_0. \quad (3)$$

The direct relaxation from $k=0$ UP to LP states is strongly inhibited for the negative detuning case considered here, even when the energy difference between the two polariton branches coincides with that of a LO phonon.^{17,18} Intermediate quasiparticles (“bottleneck” polaritons) can reach a high population due to rapid relaxation processes from high-energy states. Thus, the effective interaction between optically active polaritons and excitonlike polaritons in the bath can be assumed to be modulated by the presence of those bottleneck quasiparticles. For composite environments, where extra degrees of freedom modulate the interaction between a quantum system of interest and a large reservoir, an effective non-Markovian behavior on the quantum system dynamics arises even when the reservoir itself can be described in the Markovian approximation.¹⁹ Following this line of thought, we shall consider that polaritons optically pumped at the UP branch rapidly accumulate into an intermediate or bottleneck region of quasiparticles.¹⁷

The exact quantum evolution of the fast relaxing polariton system is far from describable in simple terms and a detailed theory of its evolution is not yet available. We can, however, fill this gap with the reasonable hypothesis that, under high intensity pumping, the intermediate polaritons can be described by a parametric approximation by using classical fields instead of full quantum field operators. This approximation ignores quantum fluctuations in the intermediate polariton fields. Thus, in H_{XP} , the $c_{\vec{k}_1}^{\dagger} c_{\vec{k}_2}$ operator is replaced by the c -number $\langle c_{\vec{k}_1}^{\dagger} c_{\vec{k}_2} \rangle \sim h_{\vec{k}_1}(t) \delta_{\vec{k}_1, \vec{k}_2}$ with $h_{\vec{k}}(t)$ acting as an effective pump on the intermediate polaritons, depending on the actual pumping pulse at the UP branch. It can be shown²⁰ that for a wide class of phase-mixed states of the pump modes identical results for the signal population can be obtained as for a coherent population of those modes. In this context, an effective classical intensity sets the system-reservoir coupling strength. Consequently, the polariton-polariton interaction term adopts the time-dependent effective form

$$H_{XP}(t) = \sum_{\vec{k}, \vec{k}'} V(\vec{k}, \vec{k}', t) a_{\vec{k}}^\dagger b_{\vec{k}'}^\dagger + \sum_{\vec{k}, \vec{k}'} V^*(\vec{k}, \vec{k}', t) a_{\vec{k}} b_{\vec{k}'}, \quad (4)$$

where

$$V(\vec{k}, \vec{k}', t) = \sum_{\vec{k}_1, \vec{k}_2} \tilde{V}(\vec{k}, \vec{k}', \vec{k}_1, \vec{k}_2) h_{\vec{k}_1}(t) \delta_{\vec{k}_1, \vec{k}_2}. \quad (5)$$

Pump depletion is determined by the interplay between the shape/length of the excitation laser pulse and polariton relaxation mechanisms in the microcavity. We shall return to this point later. The effective Hamiltonian describing the coupling of trapped polaritons ($a_{\vec{k}}$ modes) with the high-energy polariton bath ($b_{\vec{k}}$ modes), Eq. (4), corresponds to a coupling strength $V(\vec{k}, \vec{k}', t)$, which is now adjustable experimentally by varying the excitation pulse parameters such as their width and intensity. Thus, it is already clear from the present discussion how an optically controlled mechanism may exist to turn on and off memory effects in a polariton system.

Additionally, the above description explains why a Born-Markov based theoretical approach should be invalid in the present context: (i) even if the optically active polariton system is weakly coupled to the high-energy polariton reservoir, a *time-dependent* coupling strength yields to a nonexponential decay; (ii) by continuously increasing the pump-pulse intensity a strongly coupled system-reservoir situation should be reached beyond a certain threshold, hence a theory based on a lowest-order perturbation in the coupling strength breaks down; (iii) the idler-polariton bath, as being formed by higher energy polaritons (massive excitonlike particles) with a quadratic dependence of $\omega(k)$ on k , constitutes a highly structured continuum, for which a single characteristic correlation time cannot be identified.

It is worth noting that the Hamiltonian in Eq. (1), with H_{XP} as given by Eq. (4), corresponds to a nondegenerate parametric amplifier for massive particles, where the parametric gain implies that the LP population, as well as the polariton bath population, are amplified at the expense of intermediate polariton depletion. We emphasize that we are considering a pulsed excitation, thus no indefinite gain will arise and the validity of the parametric approximation is still guaranteed. Furthermore, for a time-independent system-reservoir coupling, our problem can be solved exactly. We use this to check our numerical results later.

Before we address the full numerical solution of the proposed model, an analytically tractable method is to be discussed first. This discussion is presented here because it complements the results of the microscopic treatment to be detailed below and it will also serve as a reference point.

B. Time-convolutionless non-Markovian master equation

The first type of approximation we consider is based on a semianalytical approach by using a Lindblad-type master equation with time-dependent rates allowing non-Markovian effects to be included.²¹ We start by considering a bipartite system conformed on one hand by the optically active polaritons $\vec{k} \sim 0$ and on the other hand by a high-energy polariton bath. The underlying physics is analogous to the para-

metric downconversion processes in nonlinear optics, hence consequently with an *antirotating-wave*-like coupling between those subsystems. For an initially empty polariton bath, the masterlike equation for the reduced density operator of optically active (signal) polaritons is

$$\begin{aligned} \frac{\partial \rho_S(t)}{\partial t} = & -\frac{i}{2} S(t) [a_0^\dagger a_0, \rho_S(t)] \\ & + \frac{1}{2} \gamma(t) [-a_0 a_0^\dagger \rho_S(t) - \rho_S(t) a_0 a_0^\dagger + 2a_0^\dagger \rho_S(t) a_0]. \end{aligned} \quad (6)$$

Time-convolutionless master equations of the latter form have been largely documented.²¹ The time-dependent parameters $S(t)$ and $\gamma(t)$ denote effective Lamb shift and decay rates, respectively. They are directly dependent on the reservoir spectral density.²² Equation (6) is local in time but contains all the information about memory effects in the time-dependent parameter $\gamma(t)$.

From this master equation it is immediate to obtain the equation of motion for $n(t) = \text{Tr}_S[\rho_S(t) a_0^\dagger a_0]$, the population of optically active polaritons,

$$\frac{dn(t)}{dt} = \gamma(t) [n(t) + 1]. \quad (7)$$

Given that initially the $\vec{k}=0$ mode is empty, $n(0)=0$, we found that the number of optically active polaritons grows as

$$n(t) = e^{\int_0^t \gamma(t') dt'} - 1. \quad (8)$$

In the Markov regime for which $\gamma(t) = \gamma_M = \text{constant}$, the polariton population grows exponentially. However, non-Markovian effects are evident when the relaxation rates in the master equation are time dependent. Up to now, no dissipation effects have been included in our discussion. Thus, the polariton population in the optically active mode does not cease to steadily increase. Polariton-polariton interactions, creating scattered quasiparticles out of the $\vec{k} \sim 0$ zone, cavity losses and recalling that the system-bath coupling is pulsed for a finite period of time (no continuous pumping mechanism replenishing the intermediate polariton zone is present), produce finally that $n(t)$ temporally saturates and then goes to 0. Nevertheless, any oscillation associated with the time-dependent rate $\gamma(t)$ should manifest itself not only in the rise- but also in the decay-evolution of the optically active polariton density.

One noteworthy feature of this treatment is the possibility of clarifying the growth of $n(t)$ at early times. In the Markov approximation, $n(t) = e^{\gamma_M t} - 1$, thus at short times the polariton population starts growing with a linear slope. Since a signature of non-Markovian behavior is a time-dependent relaxation rate, which starts growing as $\gamma(t) \sim gt$ (g is the system-environment coupling strength), the polariton population should behave at short times as $n(t) \sim e^{gt^2/2} - 1 \sim gt^2/2$, in qualitative agreement with the experimental results referring to the curvature of the initial time evolution (see below).

Despite the exact solvability of this model a systematic approach for dealing with mechanisms of polariton interactions and losses is not easily implementable, which makes the present formalism inadequate to describe the nonmonotonic dependence of tr-PL signals. We consider, therefore, an analytical solution of the microscopic Heisenberg dynamics to investigate in a more detailed way memory effects in polariton systems.

C. Heisenberg-Langevin dynamics

From the previous analysis, it is apparent that there is a large amount of theoretical insight to be gained from a more exhaustive examination of the proposed model. Now, a thorough formal analysis of the proposed polariton dynamics is performed. We solve directly the Heisenberg equation of motion for a given operator A . In particular, for $a_{\vec{k}}$ and $b_{\vec{k}}^\dagger$ we obtain

$$i\dot{a}_{\vec{k}} = E(\vec{k})a_{\vec{k}} + \sum_{\vec{k}'} V(\vec{k}, \vec{k}', t)b_{\vec{k}'}^\dagger + 2V_0a_0^\dagger a_0 \delta_{\vec{k},0}, \quad (9)$$

$$ib_{\vec{k}}^\dagger = -\omega(\vec{k})b_{\vec{k}}^\dagger - \sum_{\vec{k}'} V^*(\vec{k}, \vec{k}', t)a_{\vec{k}'}. \quad (10)$$

In order to solve numerically the coupled equations of motion, Eqs. (9) and (10), we formally integrate $b_{\vec{k}}^\dagger(t)$ in Eq. (10), then inserted in Eq. (9), to get

$$\begin{aligned} \dot{a}_{\vec{k}} = & -iE(\vec{k})a_{\vec{k}} - i\sum_{\vec{k}'} V(\vec{k}, \vec{k}', t)b_{\vec{k}'}^\dagger(0)e^{i\omega(\vec{k}')t} \\ & + \int_0^t \sum_{\vec{k}', \vec{k}''} V(\vec{k}, \vec{k}', t)V^*(\vec{k}', \vec{k}'', t-\tau)a_{\vec{k}''}(t-\tau)e^{i\omega(\vec{k}')\tau}d\tau \\ & - 2iV_0a_0^\dagger a_0 \delta_{\vec{k},0}. \end{aligned} \quad (11)$$

For the sake of simplicity we take $\vec{k}'' = \vec{k}$ and assume that the effective interaction V can be separated as $V(\vec{k}, \vec{k}', t) = g(\vec{k}, \vec{k}')h(t)$, where $g(\vec{k}, \vec{k}')$ accounts for both the Coulomb and Pauli effects in the polariton-polariton scattering while $h(t)$, a dimensionless real function of time, represents an effective pump-polariton pulse. As a consequence, Eq. (11) can be rewritten as

$$\begin{aligned} \dot{a}_{\vec{k}} = & -i[E(\vec{k}) - i\Gamma_0 + 2V_0a_0^\dagger a_0 \delta_{\vec{k},0}]a_{\vec{k}} - i\eta_{\vec{k}}(t) \\ & + \int_0^t h(t)h(t-\tau)a_{\vec{k}}(t-\tau)K_{\vec{k}}(\tau)d\tau, \end{aligned} \quad (12)$$

in terms of the kernel function

$$K_{\vec{k}}(\tau) = \sum_{\vec{k}'} g(\vec{k}, \vec{k}')g^*(\vec{k}', \vec{k})e^{i\omega(\vec{k}')\tau} \quad (13)$$

and a polariton-bath noise function

$$\eta_{\vec{k}}(\tau) = \sum_{\vec{k}'} g(\vec{k}, \vec{k}')b_{\vec{k}'}^\dagger(0)e^{i\omega(\vec{k}')\tau}h(\tau). \quad (14)$$

Since the memory time of the radiation field outside the microcavity is extremely short, on the order of $1/E_{\text{gap}} \sim 1$ fs

for typical II-VI gap energies $E_{\text{gap}} \sim 2-3$ eV, we are justified to treat radiation losses from the microcavity within the Markov approximation with the simple inclusion of a phenomenological damping term Γ_0 in Eq. (12). However, of primary interest here are the non-Markovian effects coming from the strong coupling between signal and idler-bath polaritons. Equation (12) embodies the memory effects on the dynamics of the emitting polaritons. The term $g(\vec{k}, \vec{k}')$ describes the strength and spectral form of the signal-idler coupling.

We emphasize that, in our model, the bath is formed by high-energy polaritons (excitonlike quasiparticles), hence the idler bath we are considering consists of massive particles. In this sense, the present signal-idler polariton coupled system is very similar to atom-laser systems with a continuous output coupler.^{22,23} However, the main difference with atom lasers is that in our case the signal-idler outcoupling is of an antirotating-wave kind [see Eq. (4)] instead of the standard rotating-wave approximation usually employed in atomic systems. In order to proceed, we assume a quadratic energy dispersion relation for the idler particles, $\omega(k) = k^2/2M_X$ with M_X the bare exciton effective mass, and a Gaussian-like profile for the trapped ground-state polariton in k -space. Consequently, the signal-idler coupling $g(\vec{k}, \vec{k}')$ can be written (in the continuum approximation for idler particles) as^{22,23}

$$g(\vec{k}, \vec{k}') = \frac{i\Gamma^{1/2}}{(2\pi\sigma_k^2)^{1/4}} e^{-(\vec{k}-\vec{k}')^2/4\sigma_k^2}, \quad (15)$$

where $\Gamma^{1/2}$ and σ_k settle the strength and width of the system-reservoir coupling, respectively. The kernel term, for the optically active mode $k \sim 0$, becomes

$$K_0(\tau) = \frac{\Gamma}{\sqrt{1-i\alpha\tau}}, \quad (16)$$

where $\alpha = \frac{\sigma_0^2}{M_X}$. Note that in our model, the bath is assumed to be formed by bosons with a dispersion relation $\omega(k) = k^2/2M_X$. This fact gives rise to distinct features in the spectral bath response and consequently in the reduced system dynamics, as compared with that found for nonmassive and structureless baths, such as those corresponding to photons or phonons.

The noise term is responsible for initiating the polariton relaxation toward the bottom LP states. Thus, we adopt for this term the role of a classical seed and have checked numerically that a very small value for it does not affect the results.

At this point we have completed the presentation of our theoretical framework and the underlying approximations, thus we can now proceed to evaluate the time evolution of the mean number of emitting polaritons at the bottom of the lower polariton branch to compare it with tr-PL experimental data.

III. RESULTS

A. Experiments

The sample under study is a $\text{Cd}_{0.4}\text{Mg}_{0.6}\text{Te}$ λ -cavity, with top (bottom) distributed Bragg reflectors (DBRs) built with

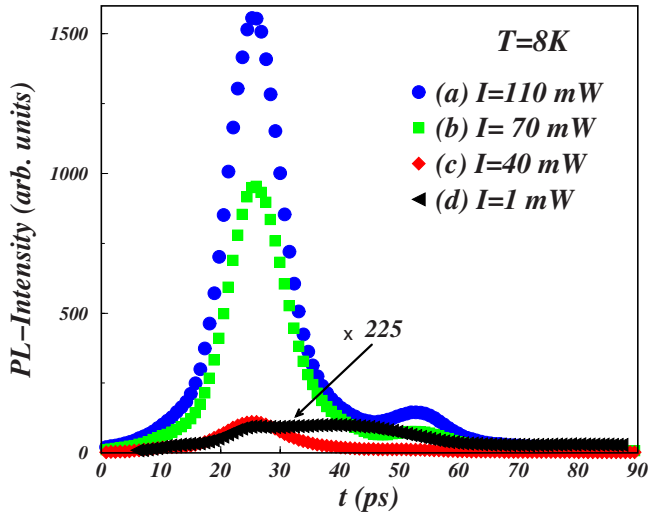


FIG. 2. (Color online) Experimental cocircularly polarized tr-PL signals for a detuning $\delta = -10$ meV at 8 K and different pulse laser intensities: $I = 110$ mW (blue circles), $I = 70$ mW (green squares), $I = 40$ mW (red diamonds), and $I = 1$ mW (black triangles).

17.5 (23) pairs of alternating $\lambda/4$ thick layers of $\text{Cd}_{0.4}\text{Mg}_{0.6}\text{Te}$ and $\text{Cd}_{0.75}\text{Mn}_{0.25}\text{Te}$. In each of the two antinodes of the electromagnetic field confined in between the DBRs there are two CdTe quantum wells (QWs) of 90 Å thickness. The strong coupling between the excitons confined in the QWs and the photons confined in the cavity yields to a Rabi splitting of ~ 10 meV at low temperature. One important parameter to be considered is the detuning $\delta = E(0) - \omega(0)$. The cavity thickness varies across the wafer, allowing to tune the photon in and out of resonance with the excitons, thus varying the detuning.

The sample is kept inside a cold-finger cryostat at a temperature of 8 K and is resonantly excited with 2 ps-long pulses derived from a Ti:sapphire laser with a 82 MHz repetition rate, impinging on the sample's surface (spot diameter 50 μm) at $\sim 3^\circ$. The excitation energy is tuned to the UP branch in order to study the coupling to the LP intermediate states, in the vicinity of the relaxation bottleneck, without involving many phonon-assisted scattering events. This resonant excitation setting allows us to simultaneously study alternative pumping configurations to the usual nonresonant excitation at the first minimum of the stop band, in order to achieve a high population at $k=0$ LP states. However it should be mentioned that similar oscillations in the tr-PL signal to those reported here have been observed after non-resonant excitation.^{9,11} The time evolution of the PL is obtained by means of a spectrograph coupled to a streak camera (time resolution ~ 10 ps). We have selected the emission originating from $k \sim 0$ lower polariton states by means of a small pinhole (angular resolution $\sim 1^\circ$). For polarization-resolved measurements we have used two $\lambda/4$ plates to excite and analyze the PL into its co/cross-circularly polarized components, after excitation with σ^+ -polarized pulses.

Figure 2 shows typical experimental cocircularly polarized tr-PL data for different laser intensities of $I = 1, 40, 70$ and 110 mW but the same detuning $\delta = -10$ meV. For the quoted laser spot size an excitation power of 1 mW corresponds to

an excitation power density of 0.05 kW/cm². The maximum of the PL signal increases in a nonlinear manner with the pulse laser intensity (note that for the weakest intensity $I = 1$ mW, the curve has been amplified by a factor of 225). New features developing on the decay side of the PL are clearly observed, with a temporal behavior dependent on the pump laser intensity. In particular, the emergence of a revival of the decaying PL signal is markedly evident for high laser intensities. This new peak becomes clearer for high intensity pumping. For positive detunings the extra peak on the decay side of the tr-PL is not present (results not shown). These observed intensity-dependent features can be fitted with good quantitative agreement using our theoretical model with memory effects controlled by the pulsed pump intensity.

B. Discussion

From the theoretical side our aim is to calculate the time evolution of the mean number of polaritons in the optically active $\vec{k}=0$ state, i.e., $\langle a_0^\dagger a_0 \rangle(t)$, by numerically solving Eq. (12). The parameters used correspond to CdTe microcavities with an exciton mass $M_X = m_e + m_h = (0.096 + 0.51)m_0 = 0.606m_0$.²⁴ We consider only heavy-hole excitons coupled to the cavity mode.

The relaxation of UP-resonantly created polaritons can be qualitatively described as follows: The direct relaxation to the LP states is strongly inhibited and the majority of polaritons scatter to large- k LP states. The situation is similar to that obtained after nonresonant excitation, i.e., there is a large polariton population at the LP bottleneck; from there polaritons relax to $k \sim 0$ states via polariton-polariton parametric scattering. We assume that the accumulation of intermediate or bottleneck polaritons, following the actual laser pulse, takes place for a longer period of time (tens of picoseconds) than the exciting pulse width (~ 2 ps), corresponding to an asymmetrical shape. Thus, it is to be modeled by an effective pump-polariton field of the form $h(t) = At^3 e^{-\beta t}$, where β can be associated with the accumulation rate of intermediate polaritons. This assumption is justified since time-resolved PL in such CdTe microcavities, under pulsed excitation, has a clear asymmetrical shape with typical decay times on the order of $10^1 - 10^2$ ps. We will call as the effective intensity, the square of the time integral of the polariton-pump pulse, $I_{pp} \sim |A\beta^{-4}|^2$, where dimensionless I_{pp} is assumed to be directly linked to the intensity of the laser pulse, I , and will enable us to connect the real excitation pump intensity with the intermediate-polariton-pump classical field. In all cases reported below, we focus on the analysis of copolarized signals, i.e., the excitation is σ^+ -polarized and the emission is analyzed into its σ^+ -polarized component.

The parametriclike interaction [see Eq. (4)], giving rise to the simultaneous creation of a $\vec{k}=0$ polariton and a bath polariton, is favored by taking negative values of δ . Besides that, tr-PL experimental results show unconventional oscillatory features in copolarized signals only for negative values of the detuning.²⁵ Consequently, we restrict our discussion and comparison with experimental data to the $\delta < 0$ case.

Figure 3 shows the high intensity experimental tr-PL signals from Fig. 2 (symbols, now independently normalized to

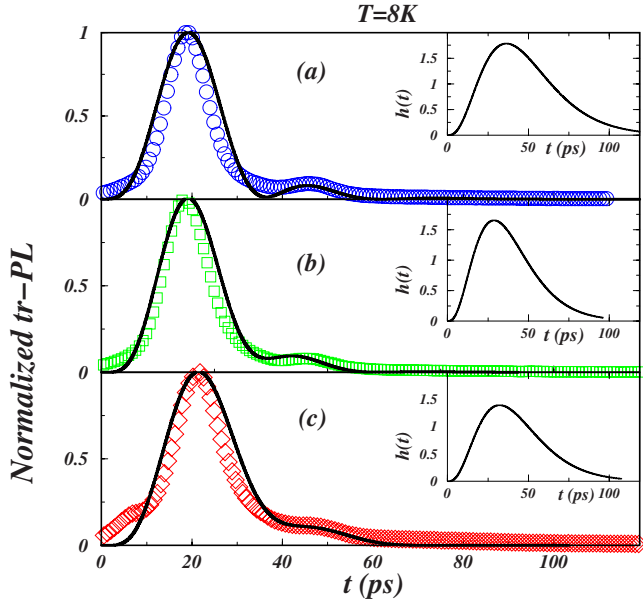


FIG. 3. (Color online) Experimental tr-PL normalized signal for different pump intensities (symbols) at 8 K and theoretical fits (continuous lines). Experimental pulse laser intensities: (a) $I = 110$ mW, (b) $I = 70$ mW, and (c) $I = 40$ mW. The insets represent the effective pump-polariton pulses $h(t)$. For theoretical parameters, see the text.

their maximum value for each pulse intensity), with the corresponding fits (solid lines) to our memory-based theory. A nonoscillatory decay is obtained in the weak pump limit or when memory effects are neglected (see below). We therefore focus on the high intensity laser pumping cases. The memory kernel $K_0(\tau)$ depends on the coupling function $g(\vec{k}, \vec{k}')$ through its width (in k -space) σ_0 and strength $\Gamma^{1/2}$. We use the following fitting parameters: $\delta = -10$ meV, $\sigma_0 = 25.7 \times 10^7$ m $^{-1}$, $\Gamma = 3 \times 10^{24}$ s $^{-2}$, which together with the bare exciton mass, M_X , define a typical signal-idler coupling time scale as $t_c = e^{|\delta|/\alpha} \sqrt{|\delta|} \alpha / 4\pi\Gamma^2 \sim 10^{-10}$ s. In terms of this coupling time, the effective-pump inverse temporal width is taken as $\beta = 6/t_c$. Other parameters are $\Gamma_0 = 0.45|\delta|$ and $V_0 = 0.02|\delta|$. By adjusting the pump-polariton pulse amplitude A , which together with β determine $h(t)$ (insets in Fig. 3), in such a way to obtain the same relative ratios between the effective pump-polariton intensities, $I_{pp} = 1, 0.64, 0.36$ as those in the actual laser pulses $I = 110, 70, 40$ mW, the computed tr-PL results reproduce both qualitatively and quantitatively the experimental data. A nonlinear initial rise of the tr-PL signal, instead of a simple linear one, is a clear signature of non-Markovian behavior. Clearly, at long times the decays are similar for both high and low intensity pump levels, thus memory effects are practically unobservable in that limit. The non-Markovian effects are more visible after the accumulation of intermediate polaritons reaches its maximum value.

In order to explore additional consequences of our model, beyond the comparison with measured tr-PL data, we proceed to discuss the effects of the pump-polariton pulse parameters on the tr-PL results. Figure 4 shows simulations of tr-PL, where only variations of the polariton-pump intensities

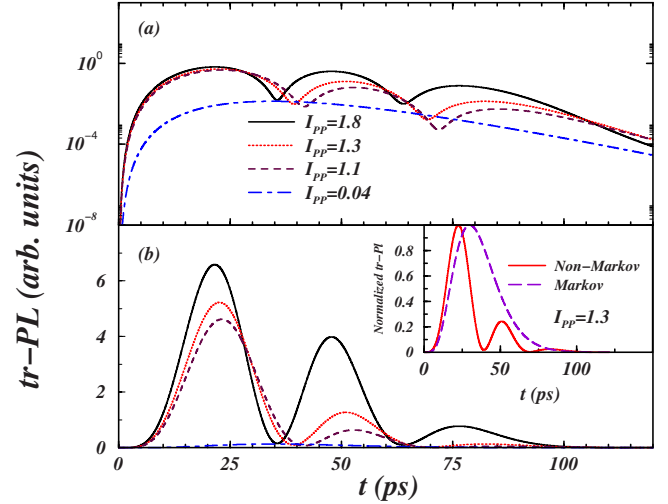


FIG. 4. (Color online) Simulated tr-PL signals for different pump-polariton intensities I_{pp} . (a) Logarithmic scale. (b) Linear scale. Inset: Comparison between Markovian (delta kernel) and non-Markovian tr-PL results for a high intensity pulse $I_{pp} = 1.3$ corresponding to a laser intensity of $I = 143$ mW.

I_{pp} are assumed [$I_{pp} = 1$ corresponds to the fitting pump intensity for the experimental curve in Fig. 3(a)]. Coupling parameters σ_0 , Γ and V_0 are identical to those used in Fig. 3. Calculated tr-PL signals are plotted in Fig. 4(a), on a logarithmic vertical scale to show the sensitivity of memory effects on the pump-polariton intensity or equivalently on the laser pulse intensity. Oscillations in the polariton population develop as the polariton-pump intensity increases. Our results clearly demonstrate that the polariton population dynamics, for a high pump excitation, shows a nonexponential (oscillatory) behavior in contrast with the typical exponential one predicted by simple Markovian approaches. In the low intensity limit a Markovian approach should be sufficient to explain the nonoscillatory behavior. This is further illustrated in Fig. 4(b), where a vertical linear scale is used to better see the evolution toward a typical Markovian signal for low intensity pumping. Furthermore, by collapsing the memory function or kernel [see Eqs. (13) and (16)] to a delta function, i.e., $K(\tau) \sim \delta(\tau)$, for a high pump intensity case, the peak on the decay side of the tr-PL disappears, as it is demonstrated in the inset of Fig. 4(b). This fact brings further support to an intensity-controlled memory mechanism in these CdTe microcavities.

One last issue to address is the sensitivity of our results on the effective pump-pulse parameters, A corresponding to the pulse height and β associated with the inverse decay time. In Fig. 5 simulated tr-PL results, for a given effective pump intensity $I_{pp} = 1$ but different pulse parameters, are depicted. We emphasize that the coupling strength between signal and idler subsystems is time dependent and goes as $\Gamma^{1/2}h(t)$. The main conclusion from Fig. 5 is that non-Markovian signatures are enhanced for an impulselike effective pump pulse, i.e., for large β or equivalently, for given I_{pp} , a large amplitude A . A nonoscillatory behavior of tr-PL signal occurs for wide pump pulses but intense and short pump pulses give rise to oscillatory patterns in tr-PL. On this basis we can

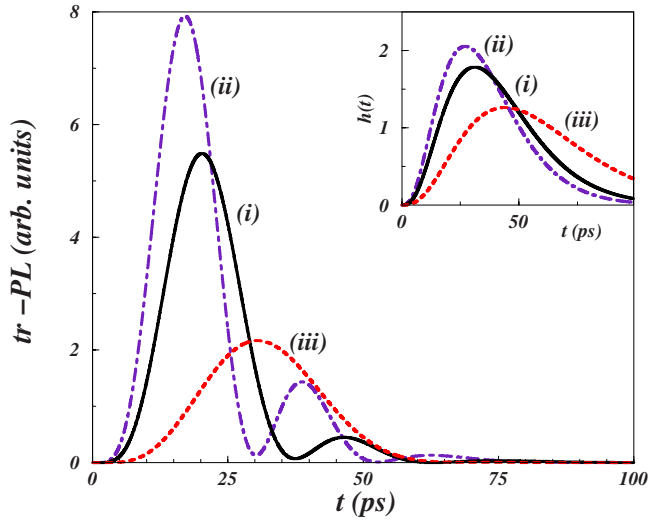


FIG. 5. (Color online) Simulated tr-PL signals for a fixed polariton-pump effective intensity $I_{pp}=1$, or equivalently $I=110$ mW, but different pulse-shape parameters: (i) Black curve (continuous line), $A=A_1$, $\beta=\beta_1$, corresponding to those parameters used in the fitting of the experimental data in Fig. 3(a). (ii) Blue curve (dashed-dotted line), $A=7A_1/4$, $\beta=(7/4)^{1/4}\beta_1$. (iii) Red curve (dashed line) $A=A_1/4$, $\beta=\beta_1/\sqrt{2}$. The inset shows the corresponding pump-pulses $h(t)$.

conclude that memory effects switch on when a high intensity pump pulse has a temporal width such that $\beta t_c^* \gg 1$, where t_c^* is an intensity-controlled coupling time given by $t_c^* = t_c/A^2$. This feature is fully consistent with our basic premises for the existence of memory effects in the sense that a large accumulation rate of intermediate polaritons would lead to a strong coupling between signal and idler (bath) polaritons. Moreover, our results suggest new possibilities for indirectly monitoring the rapid relaxation of UP polaritons to LP states. Non-Markovian effects in tr-PL could be interpreted as a signature of a rapid relaxation dynamics from nonresonantly pumped polaritons to optically active lower branch polaritons.

Markovian theories give temporal broader tr-PL signals and no oscillations are observed. Previous theoretical treatments¹² have attributed those oscillations to the existence of other states as dark excitons or spin-split states. Our theoretical analysis shows that oscillations in the tr-PL can be also produced by non-Markovian effects coming from the coupling between the trapped optically active polaritons with a polariton bath via a modulated parametriclike interaction. Furthermore, the wide range of intensities for which a satisfactory agreement is obtained demonstrates that our theoretical model indeed captures the main physics of the pulsed response of polaritons in such II-VI SM as due to

memory effects, without the need for invoking other states as responsible for those oscillations, as required by Markovian theories.

Finally, it is worthwhile to mention that spin effects are important in the polariton physics for such II-VI SM. For the cross-polarized case, i.e., excitation σ^+ -polarized and emission analyzed into its σ^- component, the same set of parameters fitting a copolarized case, for identical detuning and pump intensity, does not fit the experimentally observed results. This evidences that in this case the spin dependent polariton scattering must be properly included to describe the observed data.

IV. CONCLUSIONS

In summary, we have demonstrated that non-Markovian or memory effects produce oscillatory features in tr-PL signals in II-VI SM. In particular, we have found that the non-linear rise and the revival of the decaying PL signal for high laser intensities is explained in terms of a non-Markovian behavior of the optically active polariton system as a consequence of being efficiently coupled to a structured reservoir. These new features are enhanced in the high-laser-power excitation case. The shape and temporal width of a pump laser pulse should lead to control the dynamics of relaxing polaritons from a resonant initial distribution in the UP to access optically active states in the LP branch. Experiments to investigate this control effect would provide valuable insight into polariton dynamics and are feasible with current technology.

It is important to note, that while the tr-PL signal does not give a definite answer to the question about the exact intermediate states of the relaxation process from the initially created UP polaritons, the qualitative and quantitative agreement with the tr-PL experimental results, as a function of the excitation intensity, are strong indications of the validity of the present model. A full quantum treatment of the intermediate polariton states would be desirable. These analyses, which require considering a much more complex quantum state space, are left for further investigations.

ACKNOWLEDGMENTS

L.Q. would like to acknowledge MEC (Spain) for a sabbatical grant and the Universidad Aut3noma de Madrid-Spain for hospitality. F.J.R. and L.Q. were partially supported by research project funds from Facultad de Ciencias-Uniandes. M.D.M. thanks the Ram3n y Cajal Program. This work was partially supported by the Spanish MEC (Grants No. MAT2005-01388, No. NAN2004-09109-C04-04, and No. QOIT-CSD2006-00019), and the CAM (Grant No. S-0505/ESP-0200).

- ¹Special issue on Microcavities, edited by J. J. Baumberg and L. Viña, *Semicond. Sci. Technol.* **18**, 10 (2003).
- ²Special issue on Microcavities, edited by B. Deveaud, *Phys. Status Solidi B* **242**, 11 (2005).
- ³J. Kasprzak, M. Richard, S. Kundermann, A. Baas, P. Jeambrun, J. M. J. Keeling, F. M. Marchetti, M. H. Szymaska, R. André, J. L. Staehli, V. Savona, P. B. Littlewood, B. Deveaud and Le Si Dang, *Nature (London)* **443**, 409 (2006).
- ⁴J. Kasprzak, M. Richard, A. Baas, B. Deveaud, R. André, J. Ph. Poizat and Le Si Dang, *Phys. Rev. Lett.* **100**, 067402 (2008).
- ⁵R. Balili, V. Hartwell, D. Snoko, L. Pfeiffer, and K. West, *Science* **316**, 1007 (2007).
- ⁶C. W. Lai, N. Y. Kim, S. Utsunomiya, G. Roumpos, H. Deng, M. D. Fraser, T. Byrnes, P. Recher, N. Kumada, T. Fujisawa, and Y. Yamamoto, *Nature (London)* **450**, 529 (2007).
- ⁷S. Kundermann, M. Saba, C. Ciuti, T. Guillet, U. Oesterle, J. L. Staehli, and B. Deveaud, *Phys. Rev. Lett.* **91**, 107402 (2003); S. Savasta, O. Di Stefano, V. Savona, and W. Langbein, *ibid.* **94**, 246401 (2005); W. Langbein, *Phys. Status Solidi B* **242**, 2260 (2005).
- ⁸A. Alexandrou, G. Bianchi, E. Péronne, B. Hallé, F. Boeuf, R. André, R. Romestain, and L. Si Dang, *Phys. Rev. B* **64**, 233318 (2001).
- ⁹L. Viña, R. André, V. Ciulin, J. D. Ganiere, and B. Deveaud, *Semicond. Sci. Technol.* **19**, S333 (2004).
- ¹⁰M. D. Martin, G. Aichmayr, L. Viña, and R. André, *Phys. Rev. Lett.* **89**, 077402 (2002).
- ¹¹G. Aichmayr, M. D. Martin, and R. André, *Semicond. Sci. Technol.* **18**, S368 (2003).
- ¹²I. Shelykh, L. Viña, A. V. Kavokin, N. G. Galkin, G. Malpuech, and R. André, *Solid State Commun.* **135**, 1 (2005).
- ¹³For a review, see, C. Ciuti, P. Schwendimann, and A. Quattropani, *Semicond. Sci. Technol.* **18**, S279 (2003), and references therein.
- ¹⁴D. Porras, C. Ciuti, J. J. Baumberg, and C. Tejedor, *Phys. Rev. B* **66**, 085304 (2002).
- ¹⁵D. Porras and C. Tejedor, *Phys. Rev. B* **67**, 161310(R) (2003).
- ¹⁶F. J. Rodríguez, L. Quiroga, C. Tejedor, M. D. Martin, and L. Viña, *28th International Conference on the Physics of Semiconductors*, edited by W. Jantsch and F. Schäffler, AIP Conf. Proc. No. 893, (AIP, New York, 2007), p. 1151.
- ¹⁷J. Bloch and J. Y. Marzin, *Phys. Rev. B* **56**, 2103 (1997).
- ¹⁸A. Fainstein, B. Jusserand, and R. André, *Phys. Rev. B* **57**, R9439 (1998).
- ¹⁹A. Budini and H. Schomerus, *J. Phys. A* **38**, 9251 (2005).
- ²⁰L. Quiroga and C. Tejedor (unpublished).
- ²¹H. P. Breuer and F. Petruccione, *The Theory of Open Quantum Systems* (Oxford University Press, Oxford, 2007).
- ²²H. P. Breuer, D. Faller, B. Kappler, and F. Petruccione, *Phys. Rev. A* **60**, 3188 (1999).
- ²³G. M. Nikolopoulos, P. Lambropoulos, and N. P. Proukakis, *J. Phys. B* **41**, 025301 (2008).
- ²⁴C. Gourgon, Le Si Dang and H. Mariette, *J. Cryst. Growth* **159**, 537 (1996).
- ²⁵M. D. Martin, D. Ballarini, A. Amo, L. Viña, and R. André, *Superlattices Microstruct.* **41**, 328 (2007); M. D. Martin, D. Ballarini, A. Amo, L. Viña, and R. André, *28th International Conference on the Physics of Semiconductors*, edited by W. Jantsch and F. Schäffler, AIP Conf. Proc. No. 893 (AIP, New York, 2007), p. 1139.